Soft-Sphere DEM Simulation of Coarse Particles Transported by a Fully Developed Turbulent Gas Vertical Channel Flow

Ainur Nigmetova[1], Yann Dufresne[2], Enrica Masi[1(✉)], Vincent Moureau[2], and Olivier Simonin[1]

[1] Institut de Mécanique des Fluides de Toulouse (IMFT), Université de Toulouse, CNRS, Toulouse, France
ainur.nigmetova@toulouse-inp.fr, enrica.masi@imft.fr
[2] CORIA UMR 6614 CNRS – INSA, Université de Rouen, 76801 Saint-Etienne du Rouvray, France

Abstract. The main focus of the present study is to evaluate the accuracy of the soft-sphere method to represent the particle-particle and the particle-wall collision effect in dilute rapid particulate flow. At this aim, 3D soft-sphere Discrete Element Method (DEM) simulation results are presented for frictionless elastic and inelastic particles, for different sizes and mean solid volume fractions, transported in a fully developed vertical channel flow. The effect on particle statistics of the friction during particle-wall collisions is analyzed. Profiles of time-averaged quantities are assessed and well agree with simulation results available from the literature, obtained by using the hard-sphere model.

Keywords: Gas-particles flows · Discrete element method · Soft-sphere model

1 Introduction

Understanding the dynamics of turbulent gas–particle flows has great importance for the successful design and optimization of many industrial applications, such as fluidized beds, dust collectors, cyclone separators. These systems involve many complex mechanisms, which are often coupled and interacting with each other. In the past decades, the focus was mainly on the complexity of the interaction between particles and gas-phase turbulence [1,15] and the effect of particle–particle and particle–wall collisions [13,14].

Gas turbulence has a predominant effect on particle diffusion for small particles. In this case, the influence of the solid-solid interactions is less important, because their dynamics is controlled by the fluid motion. However, in the case of large particles, the distance they need to respond to the fluid flow is larger than the characteristic dimension of the confinement, and the effect of the flow

turbulence may be neglected. Their motion is considerably influenced by the solid-solid collision process in confined flows. In this work, the inertial particles motion in a steady and imposed fluid flow is studied.

Due to the discrete nature of the particles, the numerical simulation of the particle motion is performed in a Lagrangian framework by Discrete Element Method (DEM). Such an approach can be coupled with different models resolving the fluid phase, depending on the characteristic length scales of the fluid and particles.

An accurate resolution of particle-particle and particle-wall interactions is necessary to describe properly the whole gas-particles flow dynamics. For this reason, the objective of the present work is twofold. The first objective is to study the influence of particles properties (particle size, concentration, restitution coefficient, etc.) on the velocity statistics in vertical channel flows using the DEM simulation. For modeling the solid-solid interaction, DEM uses two approaches, the hard-sphere [3] and the soft-sphere models [5]. The soft-sphere model has computational advantages in simulating dense suspensions with multiple particle-particle contacts, while the hard-sphere model is better suited to dilute regimes. Indeed, the soft-sphere models makes it possible to address multiple collisions which occur in denses regimes, allowing particles to deform slightly at the contact point. The hard-sphere approach assumes instead that no deformation occurs during the instantaneous collision between the two solid bodies. In this work, the soft-sphere model is used, since this can treat both low and high particle number densities, and it can handle multiple contacts. Thus, the second objective is to evaluate the accuracy of the soft-sphere model to reproduce the solid-solid collision effect in a rapid gas-particles flow with dilute suspension of massive particles, comparing with Lagrangian simulation results based on the hard-sphere model [7, 9, 10].

2   General Description

2.1   Flow Configuration

The proposed test case is a gas-particles vertical fully developed channel flow, studied early by [7, 9, 10]. The corresponding Reynolds number of the fully developed flow in the channel is about 42000. The computational domain is a rectangular box, with periodic boundary conditions in the spanwise (x) and streamwise directions (z) (see Fig. 1), while the y direction is normal to the walls. A monodisperse particle-laden fluid is introduced in the vertical direction z. The physical characteristics of the fluid are $\rho_f = 1.205$ kg.m^{-3}, $\nu_f = 1.515 \times 10^{-5}$ m^2.s^{-1}. For the dispersed phase, two kinds of particle are studied: $d_p = 1.5$ mm and $\rho_p = 1032$ kg.m^{-3}, or $d_p = 406$ μm and $\rho_p = 1038$ kg.m^{-3}. These simulations are carried out for mean solid volume fractions $\langle \alpha_p \rangle$ varying between 10^{-3} and 10^{-2}. Low solid volume fractions and the large particle inertia make it possible to neglect the interactions between the fluid turbulence and the particles as well as the influence of the particles on the mean fluid flow. The Stokes number $St = \tau_p u_* / L_y$ for the present problem is about 200 and 2500 for smaller and

larger particles, respectively. Here, $\tau_p = \rho_p d_p^2 / 18\mu_f$ is the particle response time, u_* is the friction velocity and L_y is the channel width. According to the Stokes number values, it turns out that $St \gg 1$, then the particles are not affected by the turbulence of the fluid. The mean fluid velocity profile is determined from a preliminary single-phase $k - \epsilon$ computation (see Fig. 2) and fixed during all the simulations.
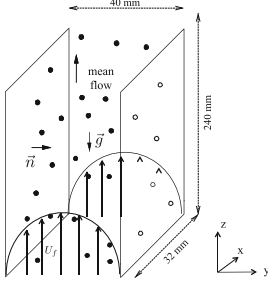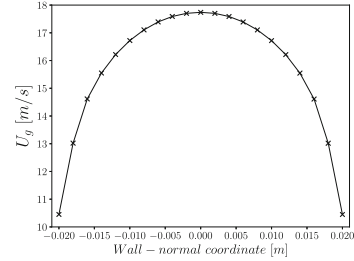

Fig. 1. Flow configuration.

Fig. 2. Mean streamwise velocity.

2.2   Averaging of Physical Quantities

Thanks to the homogeneity of streamwise and spanwise directions, mean variables depend only on the wall-normal coordinate y. Therefore, the channel is divided into 40 slices for $d_p = 406 \ \mu m$, 15 slices for $d_p = 1.5$ mm, parallel to the walls in y direction. Particles are associated with the slice in which their centres are located. The quantities are averaged spatially and temporally in each slices. The averaging operator will be written as $\langle \cdot \rangle$, $U_{p,i}$ and $u''_{p,i} = u_{p,i} - U_{p,i}$ indicate the mean velocity of the particles in the i-th direction and the velocity fluctuations, respectively. Second and third order moments are defined as following $\langle u''_{p,i} u''_{p,j} \rangle$ and $\langle u''_{p,i} u''_{p,j} u''_{p,m} \rangle$, respectively. For the sake of simplicity, the particle velocity components $(u_{p,1}, u_{p,2}, u_{p,3})$ will be written as (u, v, w), the mean velocity components $(U_{p,1}, U_{p,2}, U_{p,3})$ will be noted as (U, V, W), and the fluctuation components $(u''_{p,1}, u''_{p,2}, u''_{p,3})$ will be noted as (u'', v'', w''). And $n_p = N_p / V_c$ is defined as the particle number density, computed in a slice of volume V_c containing N_p particles.

3   Particle Dynamics: Lagrangian Simulation

The Lagrangian solver for particle tracking runs in two successive steps. The first step takes into account the fluid and gravity effects, which make move the particles. Each particle is tracked in a Lagrangian fashion based on the DEM. The fluid entrains the particles, and their velocity is changed using a second-order explicit Runge-Kutta algorithm. Since, periodic boundary conditions for particles are considered in streamwise and spanwise directions, particles leaving the calculation domain will be relocated using the periodicity and rebound

conditions. For the fluid-particles interaction, the only drag is considered. The second step deals with the inter-particle and particle-wall collisions. To compute contact between solid bodies the soft-sphere model is employed. The solids are allowed to overlap with each other in a controlled manner. The collision is detected, when the distance between two particles and between a particle and a wall is less than the sum of their radii and the radius of the particle, respectively. The collision is computed in the mass-spring-dashpot system over a time step, that must be smaller than the time step for the fluid flow. In the soft-sphere model the choice of several numerical parameters is important to solve collisions properly. Particle rotation is not taken into account in our simulations. Each step will be detailed in the following sections.

3.1   The Equations of Motion

DEM simulations is the way to simulate particulate processes, tracking each particle and considering all particle-particle and particle-wall interactions. The motion of a single spherical particle p with mass m_p is deduced from Newton's second law

$$m_p \frac{d\mathbf{u}_p}{dt} = \mathbf{F}_{D,p} + \mathbf{F}_{G,p} + \mathbf{F}_{C,p} \text{ and } \frac{d\mathbf{x}_p}{dt} = \mathbf{u}_p \tag{1}$$

$\mathbf{u}_p$ and $\mathbf{x}_p$ are the particle velocity, and position, $\mathbf{F}_{D,p}$ is the drag force, $\mathbf{F}_{G,p}$ is the gravity force and $\mathbf{F}_{C,p}$ is the collision force exerted by the neighbouring solid bodies in contact. The total collision force $\mathbf{F}_{C,p}$ acting on a particle p is computed as the sum of all the forces exerted by the N_p particles and N_w walls in contact $\mathbf{F}_{C,p} = \sum_{b=1}^{N_p+N_w} \mathbf{f}_{q \to p}^{col}$. The drag force $\mathbf{F}_{D,p}$ acting on the particle p is written

$$\mathbf{F}_{D,p} = m_p \frac{\mathbf{u}_g - \mathbf{u}_p}{\tau_{gp}} \text{ , } \tau_{gp} = \frac{4}{3} \frac{\rho_p d_p}{\rho_g C_D |\mathbf{u}_g - \mathbf{u}_p|} \tag{2}$$

where C_D is the drag coefficient. According to the assumption, the only fluid-particle interaction force taken into account is the drag. The drag coefficient is based on the Schiller and Naumann correlation [12]. And the gravitational force is written as $\mathbf{F}_{G,p} = m_p \mathbf{g}$.

For each particle, the equation of motion Eq. 1 is solved at each time step. To integrate it properly, different characteristic times based on the different phenomena (gravity, drag) are defined. Therefore, several criteria must be verified on each particle to choose the smallest time step appropriated to the most limiting characteristic time. In dilute rapid particulate flow simulations, once the stationary state is reached, the limiting time step is that defined from collision parameters.

3.2   Collision Model

Particle-particle and particle-wall collisions are modeled using the soft-sphere approach [6] originally proposed by Cundall and Strack [5]. The particles are represented as a mass-spring-dashpot system (see Fig. 3). When the distance
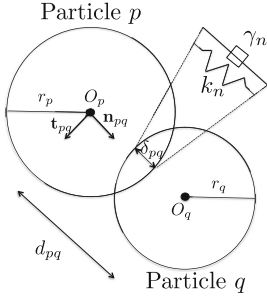
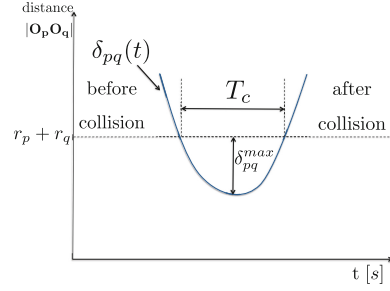**Fig. 3.** Soft-sphere representation of two particles during collision.

Fig. 4. Temporal evolution of the collision between two particles.

between particles p and q less than the sum of their radii r_p and r_q, particle starts to collide and a collision force $\mathbf{f}^{col}_{q \to p}$ is generated. This force may be decomposed in normal and tangential components. $\mathbf{f}^{col}_{q \to p} = \mathbf{f}^{col}_{n,q \to p} + \mathbf{f}^{col}_{t,q \to p}$. The normal component is computed as

$$\mathbf{f}^{col}_{n,q \to p} = \begin{cases} -k_n \delta_{pq} \mathbf{n}_{pq} - 2\gamma_n M_{pq} \mathbf{u}_{pq,n}, & \text{if } \delta_{pq} > 0 \\ 0, & \text{else} \end{cases} \tag{3}$$

where k_n is the normal spring stiffness, $\mathbf{n}_{pq}$ the normal unit vector, γ_n is the normal damping coefficient, and $\mathbf{u}_{pq,n}$ is the normal relative velocity. The term δ_{pq} is defined as the overlapping distance between two particles $\delta_{pq} = r_p + r_q - ||\mathbf{O}_p - \mathbf{O}_q||$ and $M_{pq} = (\frac{1}{m_p} + \frac{1}{m_q})^{-1}$ is the effective mass of the $p - q$ binary system. The overlapping distance is considered only in the normal direction. The unit normal vector and the normal relative velocity between particles p and q are defined respectively as

$$\mathbf{n}_{pq} = \frac{\mathbf{x}_p - \mathbf{x}_q}{||\mathbf{x}_p - \mathbf{x}_q||}, \quad u_{pq,n} = ((\mathbf{u}_p - \mathbf{u}_q) \cdot \mathbf{n}_{pq})\mathbf{n}_{pq} \tag{4}$$

where $\mathbf{u}_p$ and $\mathbf{u}_q$ are the p and q particle velocities, respectively. For the tangential component of the contact force a Coulomb-type friction law is retained $\mathbf{f}^{col}_{t,q \to p} = -\mu ||\mathbf{f}^{col}_{n,q \to p}||\mathbf{t}_{pq}$ where μ is the dynamic friction coefficient.

3.3   Collision Parameters

The projection of the Eq. 1 on $\mathbf{n}_{pq}$ gives the equation for δ_{pq} in the normal direction:

$$M_{pq} \ddot{\delta}_{pq} = -k_n \delta_{pq} - 2\gamma_n M_{pq} \dot{\delta}_{pq} \tag{5}$$

Equation 5 is the differential equation of the damped harmonic oscillator and its solution is

$$\delta_{pq}(t) = \frac{|u^0_{pq,n}|}{\sqrt{\omega_0^2 - \gamma_n^2}} \exp(-\gamma_n t) \sin(\sqrt{\omega_0^2 - \gamma_n^2} t) \tag{6}$$

with undamped angular frequency $\omega_0 = \sqrt{\frac{k_n}{M_{pq}}}$ and normal damping parameter $\gamma_n = \frac{-\ln e_n}{\sqrt{\pi^2 + \ln^2 e_n}} \omega_0$, where e_n is the normal restitution coefficient. It means that the overlap depends on the user-defined parameters k_n, e_n and the particle properties. The differentiation of Eq. 6 provides that $\dot{\delta}_{pq}(t = 0) = |u^0_{pq,n}|$. The contact during collision is solved over time and the duration of a contact can be determined as a time corresponding to the end of the collision $\delta_{pq}(t = T_c) = 0$ (see Fig. 4):

$$T_c = \frac{\pi}{\sqrt{\omega_0^2 - \gamma_n^2}} \tag{7}$$

Since, the particle phase is monodisperse, T_c has a unique value in the particulate system. The contact duration depends on ω_0, γ_n, which depend on k_n, e_n and particle properties. It is essential to estimate the appropriate collision duration to perform simulations with appropriate particle time step.

3.4   Numerical Parameters

To ensure the numerical stability for the used numerical schemes and to treat the collision properly, the particle time step Δt_p must be small enough. For example, in the case of the hard-sphere model, according to [11], where the particle velocity after collision is defined analytically from the velocity before collision, the limiting condition is defined as $\Delta t_p < \theta d_p / ||\mathbf{u}_r||$, with $\theta \approx 0.3$. The information needed to estimate this condition is the mean relative impact velocity $u_r = ||\mathbf{u}_r||$, which can be estimated from the particles agitation $q_p^2 = 1/2(u'' + v'' + w'')$

$$u_r = \sqrt{\frac{8}{3\pi} q_p^2} \tag{8}$$

In our simulations based on the soft-sphere model, to estimate the time step, several conditions must be verified. First of all, Δt_p has to be smaller or equal than the fluid time step, which is estimated from the CFL condition for the fluid phase $CFL = \max_{i=1,3} |u_{f,i}| \Delta t_f / \Delta x_f$. To choose an appropriate value for Δt_p two conditions should be verified. The first condition $CFL_p = \Delta t_p ||\mathbf{u}_p|| / \Delta x_f$ for each particle is needed to ensure that a particle does not move more than few elements of the Eulerian mesh during a substep. The second condition is based on the fact that during a substep particles do not move more than $100 \cdot CFL_p^{col}$ % of their diameter, where $CFL_p^{col} = \Delta t_p |u^0_{pq,n}| / d_p$. It means that this condition is necessary to control and limit the overlapping distance at the first impact. Another condition is that Δt_p must be inferior to the contact time T_c to limit the overlapping distance during the collisions and to reach a sufficient resolution for the time integration of the stiff collision term in Eq. 1 (see Fig. 4)

$$\Delta t_p < \frac{T_c}{N_c}. \tag{9}$$

N_c is the minimum number of steps during one contact. It is recommended in the literature to integrate a dry contact with Δt_p in the range $[T_c/50, T_c/15]$ [2], and following [8] in the gas-particles flow N_c should be greater than $N_c > 5$.

As discussed above, T_c depends on some parameters like k_n, e_n and particle properties. Then to predict the collision duration T_c, the appropriate value for k_n must be chosen for a given particle. Frequently used practice is to predict the appropriate value for k_n from the maximum value for the overlapping distance. The maximum overlap δ_{pq}^{max} is obtained from $\dot{\delta}(t) = 0$

$$\frac{\delta_{pq}^{max}}{d_p} = \frac{|u_{pq,n}^0|}{\omega_0 d_p} \exp\left(-\frac{\gamma_n}{\sqrt{\omega_0^2 - \gamma_n^2}} \arcsin \frac{\sqrt{\omega_0^2 - \gamma_n^2}}{\omega_0}\right) \qquad (10)$$

By using an estimate for the value of $u_{pq,n}^0$ and fixing the maximum overlap δ_{pq}^{max}, k_n can be obtained from Eq. 10. The only drawback of this approach is the lack of information concerning $u_{pq,n}^0$ before performing the simulations. In some references, it is recommended that the maximum overlapping δ_{pq}^{max} is less than 10% of the particle diameter [4], other references propose instead to keep its value less than 1% [8]. The resulting high value of k_n leads to a small particle time step, which is very limiting for the numerical simulation. The point is how should be evaluated the stiffness coefficient to have less constrained particle time step without significantly affecting the flow dynamics. It will be discussed in the next section.

4   Simulation Results and Discussions

DEM simulations of the vertical channel flow are here presented. They are used to study the influence of the particle properties on the velocity statistics and to evaluate the soft-sphere approach in rapid particulate flow. Numerical test cases and main parameters are presented in the Table 1. The value of relative velocity u_r for all cases is obtained from q_p^2 using Eq. 8.

Table 1. Numerical test cases.

Case	d_p	$\langle \alpha_p \rangle$	N_p	δ_{pq}^{max}/d_p	k_n	Δt_p	Δt_f	N_c	CFL_p	CFL_p^{col}	u_r
B	406 μm	1.2×10^{-3}	10520	0.05	3000 N/m	10^{-6} s	10^{-5} s	10	1.5	0.01	1.05 m/s
C	406 μm	4×10^{-3}	35067	0.05	3000 N/m	10^{-6} s	10^{-5} s	10	1.5	0.3	0.87 m/s
D	406 μm	1×10^{-2}	87668	0.05	3000 N/m	10^{-6} s	10^{-5} s	10	1.5	0.3	0.79 m/s
E	1.5 μm	4.1×10^{-3}	712	0.03	5000 N/m	4×10^{-5} s	2.5×10^{-5} s	10	1.5	0.01	0.61 m/s
F	1.5 mm	1.4×10^{-2}	2433	0.03	5000 N/m	4×10^{-5} s	2.5×10^{-5} s	10	1.5	0.3	0.56 m/s
G	1.5 mm	4.1×10^{-2}	7127	0.03	5000 N/m	4×10^{-5} s	2.5×10^{-5} s	10	1.5	0.3	0.53 m/s

Results for the mean particle streamwise velocity are shown by Fig. 5 (left panel). The fluid velocity is frozen and is the same for all studied cases (see Fig. 2). The left and middle panels of Fig. 5 correspond to the elastic frictionless cases for the inter-particle ($e_c = 1, \mu_c = 0$) and the particle-wall ($e_w = 1, \mu_w = 0$) collisions. Results show that, for all the cases, the mean particle velocity profile is flatter than that of the fluid (Fig. 2); this is due to the strong influence of transverse particle dispersion. Results also show that the mean particle velocity

is mostly dependent on the particle diameter, which in turn shows the strong influence of the drag. The mean particle number density demonstrates (see the middle panel of Fig. 5) that near-wall geometrical effects have a strong influence on the collisional characteristics and lead to an overcrowding of the particles, creating a mean force towards the wall [7, 9, 10]. Smaller particles ($d_p = 406\,\mu\text{m}$) are more transported by the fluid than larger particles ($d_p = 1.5\,\text{mm}$) at the center of the channel. Larger particles are instead more concentrated at the near wall region than the small ones. The numerical simulations results based on the soft-sphere model are in excellent agreement with hard-sphere model simulations for both mean streamwise velocity and mean particle number density (see the left and middle panel of Fig. 5). Kinetic stress components (second-order particle velocity correlations) for the case $\langle \alpha_p \rangle = 1 \times 10^{-2}$ are presented by Fig. 5 (right panel) for two different set of particles-wall collision parameters ($e_w = 1, \mu_w = 0$ and $e_w = 0.94, \mu_w = 0.325$). The difference between the elastic frictionless case and the inelastic case with friction shows the strong sensitivity of the system to the boundary conditions for particles. Inelastic restitution $e_w < 1$ induces dissipation at the wall. When $\mu_w > 0$, it causes a friction effect at the wall characterized by a non-zero value of the shear stress $\langle u''v'' \rangle$. The friction effect involves a production of the vertical variance $\langle u''u'' \rangle$ by the velocity gradient term and, by collisional redistribution, an increase in $\langle v''v'' \rangle$ and $\langle w''w'' \rangle$. In the inelastic case with friction our results also fully agree with the simulations based on the hard-sphere model [10].
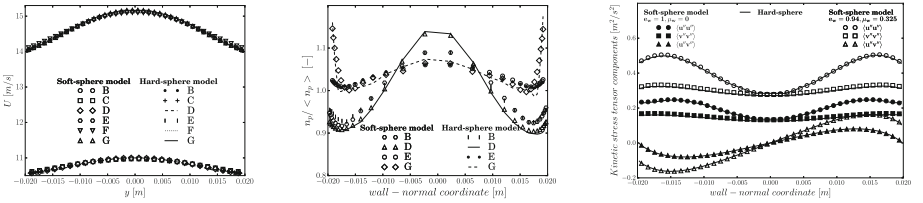

Fig. 5. Comparison between numerical simulations based on the soft-sphere and the hard-sphere model. Left: mean streamwise velocity, middle: mean particle number density, right: kinetic stress tensor components for the case D.

The stiffness coefficient sensitivity analysis is realized to evaluate the accuracy of the soft-sphere model. In order to ensure this, first, Eq. 10 can be bounded from above using $e_c \leqslant 1$ or $e_w \leqslant 1$

$$\frac{\delta_{pq}^{max}}{d_p} \leqslant \frac{|u_{pq,n}^0|}{d_p}\sqrt{\frac{M_{pq}}{k_n}} \leqslant \lambda,\ 0 < \lambda \leqslant 0.01 \tag{11}$$

for the highest value of k_n. On the other hand, $|u_{pq,n}^0| \approx k \cdot u_r$ for $k \leqslant 2$. Then, Eq. 11 will be rewritten like

$$\frac{\delta_{pq}^{max}}{d_p} \leqslant \frac{u_r}{d_p}\sqrt{\frac{M_{pq}}{k_n}} \leqslant \frac{\lambda}{k},\ 0 < \lambda \leqslant 0.01 \tag{12}$$
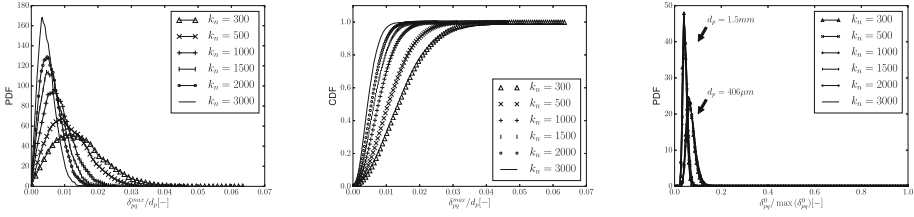
Fig. 6. Comparison for the different values of the stiffness coefficient. Left: probability density function (PDF) of the dimensionless maximum overlapping distance ($d_p = 406\,\mu\text{m}$), middle: cumulative distribution function (CDF) of the dimensionless maximum overlapping distance ($d_p = 406\,\mu\text{m}$), right: PDF of the first overlap weighted by $\max\left(\delta_{pq}^0\right)$

As shown by Fig. 6 (left pannel), the maximum value of the overlap is strongly dependent on k_n (see Eq. 10). The higher k_n, the lower the mean value of δ_{pq}^{max}/d_p will be. But it is relevant to notice that even when k_n is low ($k_n = 300$), the percentage of the collisions which have the high overlapping is very small, as shown by cumulative distribution function (see the middle panel of Fig. 6). And its mean value corresponds more to the small overlapping. The high values of δ_{pq}^{max}/d_p occurring rarely do not affect the whole dynamics of the gas-particles flow as demonstrated by Fig. 7 for different quantities. This observation provides to weaken the conditions on δ_{pq}^{max}/d_p (Eq. 11).

Moreover, from Fig. 6 (right panel), it is observed that the first distance of the overlap δ_{pq}^0 does not depend on the stiffness coefficient value for different particle diameters, the first impact relative velocity u_r does not as well. This fact allows to identify the dimensionless parameter $\kappa_n = \frac{u_r}{d_p}\sqrt{\frac{M_{pq}}{k_n}}$ depending on u_r and to estimate the mean overlapping distance as

$$\frac{\delta_{pq}^{mean}}{d_p} \leqslant \kappa_n \leqslant \lambda^* \tag{13}$$

where λ^* takes values between $(0, 0.05)$ less constraining for Δt_p. The dimensionless parameter κ_n provides the estimation of the mean overlapping knowing the value of the mean particles agitation and k_n for a given particle.
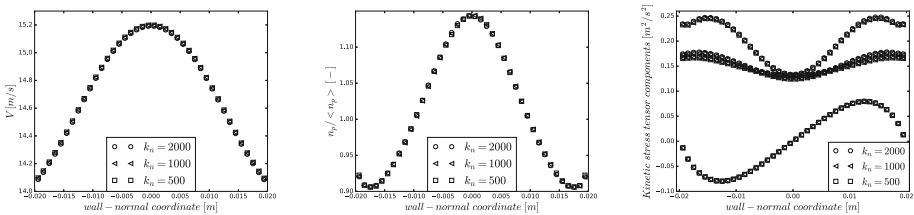

Fig. 7. Simulation results based on the soft-sphere model for different stiffness coefficients for the case D. Left: mean streamwise velocity, middle: mean particle number density, right: kinetic stress tensor components

5   Conclusion

Soft-sphere DEM simulations have been performed and numerical results analyzed for a vertical gas-particles channel flow. Simulations have been performed neglecting the influence of the fluid turbulence on the particle fluctuating motion and the modification of the fluid flow by the particles. Two types of particles have been studied, for various mean volume fractions. Results based on two approaches, the soft-sphere and the hard-sphere models, have been compared and validated quantitatively and qualitatively for different physical variables. Thereafter, a sensitivity analysis about the soft-sphere model parameters has been carried out to gain insight in the choice of the optimal ones to properly treat the solid-solid collision. It was found that a less restrictive model for the maximum overlapping distance can be defined as a function of the mean value of the impact variables without influencing the flow behaviour.

References

1. Berlemont, A., Simonin, O., Sommerfeld, M.: Validation of inter-particle collision models based on large eddy simulation. ASME-PUBLICATIONS-FED **228**, 359–370 (1995)
2. Bernard, M., Climent, E., Wachs, A.: Controlling the quality of two-way Euler/Lagrange numerical modeling of bubbling and spouted fluidized beds dynamics. Ind. Eng. Chem. Res. **56**, 368–386 (2016)
3. Campbell, C., Brennen, C.: Computer simulation of shear flows of granular material. Stud. Appl. Mech. **7**, 313–326 (1983)
4. Capecelatro, J., Desjardins, O.: An Euler-Lagrange strategy for simulating particle-laden flows. J. Comput. Phys. **238**, 1–31 (2013)
5. Cundall, P., Strack, O.: A discrete numerical model for granular assemblies. Geotechnique **29**, 47–65 (1979)
6. Dufresne, Y., Moureau, V., Masi, E., Simonin, O., Horwitz, J.: Simulation of a reactive fluidized bed reactor using CFD/DEM (Center for Turbulence Research Proceedings of the Summer Program) (2016)
7. Fede, P., Simonin, O.: Direct simulation Monte-Carlo predictions of coarse elastic particle statistics in fully developed turbulent channel flows: comparison with deterministic discrete particle simulation results and moment closure assumptions. Int. J. Multiphase Flow **108**, 25–41 (2018)
8. van der Hoef, M.A., Ye, M., van Sint Annaland, M., Andrews, A.T., Sundaresan, S., Kuipers, J.A.: Multiscale modeling of gas-fluidized beds. Adv. Chem. Eng. **31**, 65–149 (2006)
9. Sakiz, M., Simonin, O.: Continuum modelling and Lagrangian simulation of the turbulent transport of particle kinetic stresses in a vertical gas-solid channel flow. In: 3rd International Conference on Multiphase Flows, Lyon, France (1998)

10. Sakiz, M., Simonin, O.: Development and validation of continuum particle wall boundary conditions using Lagrangian simulation of a vertical gas-solid channel flow. ASME-PUBLICATIONS-FED **99** (1999)
11. Sakiz, M.: Simulation numérique Lagrangienne et modélisation eulérienne d'écoulements diphasiques gaz-particules en canal vertical. Ph.D. thesis, Marne-la-vallée, ENPC (1999)
12. Schiller, L., Naumann, A.: A drag coefficient correlation. Vdi Zeitung **77** (1935)
13. Sommerfeld, M.: Analysis of collision effects for turbulent gas-particle flow in a horizontal channel: part I. Particle transport. Int. J. Multiphase Flow **29**, 675–699 (2003)
14. Tanaka, T., Tsuji, Y.: Numerical simulation of gas solid two-phase flow in a vertical pipe on the effect of inter particle collision (1991)
15. Vreman, A.: Turbulence characteristics of particle-laden pipe flow. J. Fluid Mech. **584**, 235 (2007)